Title
Performance of Hole Coupling Resonator in the Presence of Asymmetric Modes and FEL Gain

Authors
Xie, M
Kim, K.-J.

Publication Date
1991-08-01

LBL-30672

Lawrence Berkeley Laboratory
UNIVERSITY OF CALIFORNIA

Accelerator & Fusion Research Division

Presented at the Thirteenth International Free Electron Laser Conference, Santa Fe, New Mexico, August 26–30, 1991, and to be published in the Proceedings

Performance of Hole Coupling Resonator in the Presence of Asymmetric Modes and FEL Gain

M. Xie and K.-J. Kim

August 1991

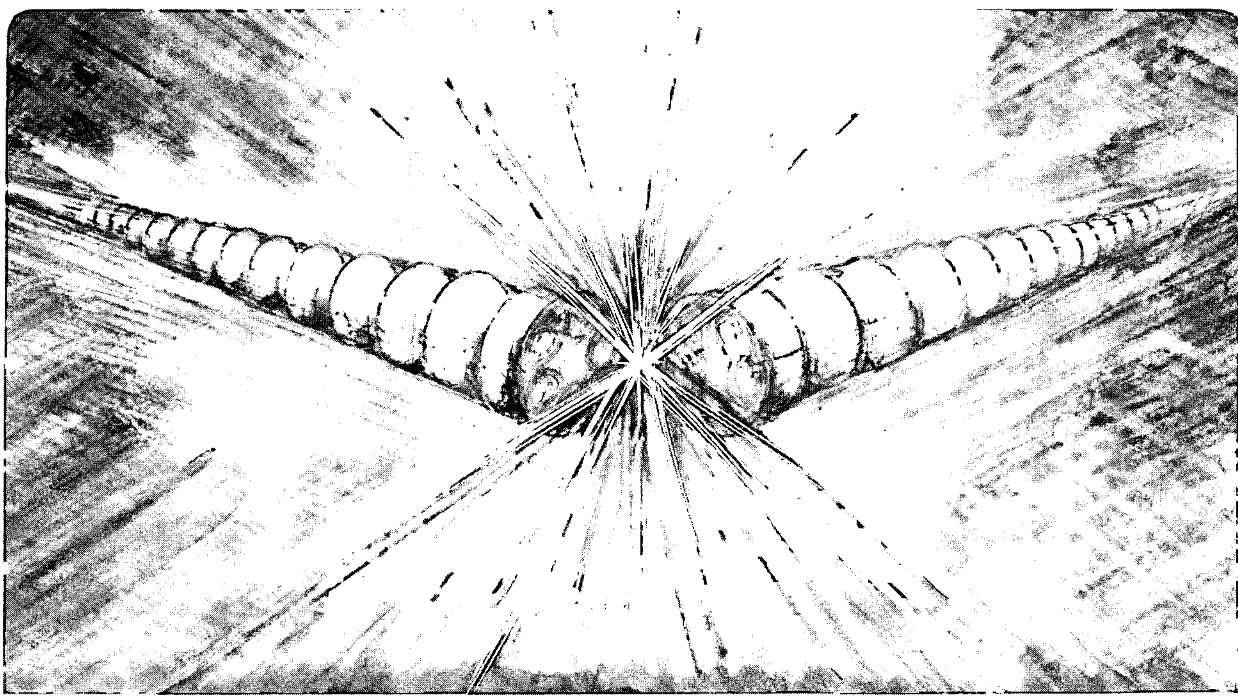

Prepared for the U.S. Department of Energy under Contract Number DE-AC03-76SF00098

DISCLAIMER

LBL-30672

ESG Note-131

PERFORMANCE OF HOLE COUPLING RESONATOR IN THE PRESENCE OF ASYMMETRIC MODES AND FEL GAIN*

Ming Xie and Kwang-Je Kim

Lawrence Berkeley Laboratory

University of California

Berkeley, CA 94720

Paper Presented at Thirteenth International Free Electron Laser Conference

Santa Fe, New Mexico, USA, August 26-30, 1991

* This work was supported by the Director, Office of Energy Research, Office of Basic Energy Sciences, Materials Sciences Division, of the U.S. Department of Energy under contract No. DE-AC03-76SF00098.

Abstract

We continue the study of the hole coupling resonator for free electron laser (FEL) application. The previous resonator code is further developed to include the effects of the azimuthally asymmetric modes and the FEL gain. The implication of the additional higher order modes is that there are more degeneracies to be avoided in tuning the FEL wavelengths. The FEL interaction is modeled by constructing a transfer map in the small signal regime and incorporating it into the resonator code. The FEL gain is found to be very effective in selecting a dominant mode from the azimuthally symmetric class of modes. Schemes for broad wavelength tuning based on passive mode control via adjustable apertures are discussed.

1. Introduction

In our previous paper [1], henceforth referred to as I, we have studied the hole coupling performance of the near concentric resonators for FEL application. The resonator configuration is shown in Fig.(1). The resonator and FEL parameters are listed in Table (1). We have used a new resonator simulation code HOLD, based on the Fox-Li iterative approach [2], to compute several performance parameters; total round-trip cavity loss, hole-coupling efficiency, output mode quality factor, etc.. We also found that the modes can become degenerate for certain cavity configurations which must be avoided for FEL operation. In this paper we extend our work to take into account the asymmetric modes, and the effect of the FEL gain on the mode formation. Our study leads to a strategy for a broadly tunable hole coupling scheme, in which an adjustable aperture is introduced to avoid the mode degeneracy.

The asymmetric modes could become important when the loss of the fundamental mode becomes large. We have modified HOLD so that the cavity performance can be calculated for an arbitrary azimuthal mode number m. The presence of the asymmetric modes limits the wavelength tuning range. However, the symmetric and asymmetric higher order modes can be suppressed by adjustable apertures, and a satisfactory solution could be found.

The approximation of neglecting the FEL gain is valid when the gain is small and when the input wave-front is modified only once through the gain medium such as in an amplifier. However, the cumulative effect of a small gain over many passes in an oscillator FEL could be significant. To include the FEL interaction in the resonator, we have modified HOLD by replacing the free-space propagation from aperture 1 to aperture 2 in Fig.(1) by an FEL transfer map. The FEL transfer map was obtained in the small signal, low gain approximation by solving a three-dimensional FEL integral equation.

The results of the hole coupling resonator study taking into account the FEL gain are as follows: For symmetric modes, the most significant result is the desirable fact that the FEL gain is very effective in suppressing the higher order modes, when the electron beam size is not too small. Otherwise, the FEL gain has little influence on the mode profile and hence the resonator performance. Also, the asymmetric modes are not significantly perturbed by FEL gain because those modes have vanishing intensity at the electron beam location. The net result is that the hole coupling performance becomes somewhat better when the FEL interaction is taken into account.

Section 2 gives a summary of I, as well as discussion of the asymmetric modes. The discussion of FEL model is given in Section 3. Section 4 presents the results of resonator calculations taking the FEL interaction into account. Section 5 contains concluding remarks.

2. Summary of Empty Cavity Performance Including Asymmetric Modes

In general, there exist a unique set of eigenmodes for a given resonator. A mode is defined to be the wave profile which reproduces itself after one round-trip propagation in the cavity, except for a multiplicative constant. The constant is called the eigenvalue of the mode. The magnitude of the mode determines the round-trip loss α_T. For resonators with cylindrical symmetry, an eigenmode can be represented by a complex amplitude $E_{mn}(r,z)$, where m and n are respectively the azimuthal and the radial mode numbers, r and z are the radial and the axial coordinates. This mode will be referred to as the TEM_{mn} mode. When there are no holes on the mirrors, the fundamental TEM_{00} mode is always the dominant one because the higher order modes extend further out radially and their losses would then be higher due to the finite mirror size. In general, the mode number n is determined by the number of minima in the radial direction. The intensity of the asymmetric modes $m \neq 0$ vanishes on the symmetry axis. Thus, the asymmetric modes are less sensitive to the presence of the holes located on the axis, as long as the hole size is not too large.

The cavity configuration under investigation is shown in Fig.(1), and consists of four elements; the right mirror with a hole, the left mirror with an adjustable aperture for mirror size control, and two intracavity apertures simulating the undulator bore. We define six fractional losses α_i as follows: The fractional losses α_{RM} and α_{LM} at the right and the left mirrors, respectively, and the fractional losses α_{R1} and α_{L1} (α_{R2} and α_{L2}) at the aperture 1 (aperture 2) for the waves coming from right and from left, respectively. The total round-trip loss α_T is then given by

$$1 - \alpha_T = \prod_i (1 - \alpha_i) \quad . \tag{1}$$

The loss α_{RM} consists of two parts, the loss through the mirror edge and the loss through the hole α_H. The coupling efficiency η is defined to be

$$\eta = \frac{\alpha_H}{\alpha_T} \quad . \tag{2}$$

The quantities α_T and η are important performance parameters of a hole coupling resonator. The definition of η here is slightly different from the previous definition [1], but has the advantage of being consistent with our new calculations with the FEL gain included. In fact a definition of coupling efficiency is an unambiguous representation of power coupling efficiency only at steady state, in which the gain in the active medium balances the losses.

The code HOLD developed in I for m=0 modes has now been generalized for the asymmetric modes for $m \neq 0$. For an arbitrary resonator configuration, the code calculates the intracavity mode profile, the eigenvalue, the coupling efficiency, and output mode quality factor for the dominant mode for each azimuthal mode number m.

We say here that two modes are degenerate when the round-trip losses are the same. Degenerate modes have in general different round-trip phase advances. An exception is for the case of a confocal resonator, for which all the radial modes with same azimuthal mode number have the same phase advances (modulo 2π) in the limit of small losses [3].

As the hole size is increased continuously, at fixed mirror sizes, we found in I that the dominant cavity mode switches abruptly from the fundamental mode to the next higher order mode. The transition occurs when the two modes have the same losses. At this point, the cavity mode is a linear combination of the two modes. Because of the difference in the round-trip phase advances (roughly a factor of three difference was found in this case between the zeroth and the first order radial mode, as expected from the phase advances in Gauss-Laguerre modes) the coefficients of the combination change from pass to pass, causing the transverse profile to oscillate in shape. It is clearly important to avoid the mode degeneracy and switching during an FEL wavelength tuning.

The situation is different in the case of confocal resonator where the transition is smooth [4]. This is related to the fact that the phase advances for different radial modes are the same for a confocal resonator, and thus a linear combination of the modes may also give a stable profile [5]. The confocal resonators are not suitable for high efficiency output coupling, since the mode could avoid the holes. We do not consider the case of confocal resonator further in this paper.

The mode switching would also occur if the hole size is fixed while the mirror size increases, and likewise if both hole and mirror sizes are fixed while the wavelength decreases. The similarity in the roles of the three controlling parameters, the wavelength, hole and mirror sizes, suggests a scheme for an extended wavelength tuning range. Thus the performance fall-off due to a wavelength change can be compensated by a suitable change in either the hole size or the mirror size. Although it is difficult to vary the hole size of a given cavity mirror, the effective mirror size can be easily changed by means of an adjustable aperture in front of the cavity mirror. (In fact our study shows that such an aperture can be placed at any convenient location inside the cavity to provide equally effective mode control.)

Figure (2) shows the wavelength dependence of the hole coupling performance for variable mirror sizes. The right mirror size is chosen to be sufficiently large while the left mirror size increases linearly from 6.7 mm to 10 mm as the wavelength is tuned from 3 to 6 μm. Note that the coupling efficiency and the loss remain close to 45 % and 10 % respectively, varying little in the range between 3 to 6 μm. Also, the loss of the TEM_{10} mode is kept to be larger than that of the TEM_{00}. Although not shown, the losses of other higher order modes are larger by our choice of the mirror size. For comparison, Fig.(3) shows the corresponding curves for the case where the left mirror size is fixed at the midpoint value of 8.35 mm. The performance is not acceptable. At short wavelength end, the mirror size appears too big so that the TEM_{10} mode is the dominant one. The TEM_{10} mode becomes degenerate with the fundamental mode at λ=4.3 μm. On the other hand, the mirror size appears too small at longer wavelength end so that the coupling efficiency is reduced.

3. Modeling the FEL with Transfer Map

Let $\mathcal{E}(\mathbf{r},z,t)$ be the electric field of the wave propagating along the z-direction. The transverse coordinates and the time are represented by $\mathbf{r}$ and t, respectively. We introduce the complex amplitude $E(\mathbf{r},z)$ by $\mathcal{E}(\mathbf{r},z,t)=E(\mathbf{r},z)e^{i(kz-\omega t)}$, where $k=2\pi/\lambda$, $\omega=ck$, c=speed of light, and λ is the radiation wavelength. The paraxial wave equation is

$$\left[\nabla^2 + 2ik\frac{\partial}{\partial z}\right]E(\mathbf{r},z) = 2ik\, S(\mathbf{r},z) \ , \qquad (3)$$

where ∇^2 is the transverse Laplacian and $S(\mathbf{r},z)$ describes a spatially distributed source. By solving Eq.(3), the field profile at $z=z_2$ along the direction of wave propagation is determined by an integral transform of the profile earlier at a location $z=z_1$ as follows:

$$E(\mathbf{r}_2, z_2) = \int d\mathbf{r}_1\, G(\mathbf{r}_2, \mathbf{r}_1, z_2, z_1)\, E(\mathbf{r}_1, z_1) + \int_{z_1}^{z_2} dz \int d\mathbf{r}\;\; G(\mathbf{r}_2, \mathbf{r}, z_2, z)\;\, S(\mathbf{r},z) \quad , \tag{4}$$

where G is the Green function of Eq.(3). In the absence of the source term, Eq.(4) reduces to the well-known Fresnel-Kirchhoff integral for the wave propagation and diffraction in free space.

In the weak field limit, the source term S for an FEL can be written to a good approximation as follows [6,7]:

$$S(\mathbf{r},z) = i g_0 \rho(\mathbf{r},z)\, e^{-i\mu z} \int_0^z dz' \int_0^{z'} dz''\, e^{-i\mu z''} E(\mathbf{r},z'') \quad , \tag{5}$$

where $\rho(\mathbf{r},z)$ is electron density profile, $\mu=\nu/L$, ν is the FEL resonance parameter defined by $\nu=L[k_u-k(1+K^2)/2\gamma^2]$, L is the length of the undulator, γ is the relativistic energy factor, $k_u=2\pi/\lambda_u$, λ_u is undulator period, K is undulator deflection parameter, and g_0 is a gain parameter proportional to the beam current. In the case of a parallel electron beam, g_0 is given by

$$g_0 = \frac{8\sqrt{2}\,\pi^2\,\lambda^{3/2}\,\lambda_u^{1/2}\,N^3\,K^2}{(1+K^2)^{3/2}\,L^3}\,\frac{I}{I_A} \tag{6}$$

where I is the beam current, N is the number of undulator period, and I_A, the Alfven current, is about 17030 Amperes. For simplicity, the undulator field is assumed to be helical. With the FEL source given by Eq.(5), Eq.(4) becomes an integral equation for the field. Taking free-space propagation term (the first term on the right-hand side of Eq.(4)) as the zeroth order, a perturbation solution can be obtained in the following form:

$$E(z) = \left[\hat{G} + g_0\hat{K} + g_0^2\hat{K}^2 + \ldots\right] E(0) \quad , \tag{7}$$

where the operator $\hat{G}$ represents the free-space transfer map, and the operator $\hat{K}^n$ represents the nth order FEL transfer map. At low gain the perturbation series can be truncated to the first order. Assuming that both resonator and electron beam are axially symmetric, Eq.(7) to the first order can be expressed explicitly in polar coordinate as

$$E_m(r,z) = \int_a^b r'dr' \left[G_m(r,r',z,0) + g_0 K_m(r,r',z,0)\right] E_m(r',0) \quad , \tag{8}$$

where $E_m(r,z)$ is the azimuthal mode of order m, a and b are radial boundaries, and

$$G_m(r,r',z,z') = \frac{(-i)^{m+1}k}{z-z'} e^{\frac{ik(r^2+r'^2)}{2(z-z')}} J_m\left(\frac{krr'}{z-z'}\right) \quad ,$$

$$K_m(r,r',z,0) = i\int_0^z dz' \int_0^{z'} dz''z''\, e^{-i\mu z''} \int_0^\infty r''dr''\, \rho(r'',z')\, G_m(r,r'',z,z')\, G_m(r'',r',z',z'') \quad . \tag{9}$$

In the above J_m is the Bessel function of order m.

It is more convenient for numerical calculations to express the first order transfer map in a different form. Introducing Hankel transform

$$\tilde{E}_m(p,z) = \int_0^\infty rdr\, J_m(pr)\, E_m(r,z) \quad , \tag{10}$$

Eq.(8) can be written in spectral domain as

$$\tilde{E}_m(p,z) = e^{-\frac{ip^2}{2k}z}\, \tilde{E}_m(p,0) + g_0 \int_0^\infty p'dp'\, \tilde{K}_m(p,p',z,0)\, \tilde{E}_m(p',0) \quad , \tag{11}$$

where

$$\widetilde{K}_m(p,p',z,0) = ie^{-\frac{ip^2}{2k}z}\int_0^z dz'\int_0^{z'} dz''\int_0^{z''} dz''' e^{i\left(\frac{p^2}{2k}-\mu\right)z'-i\left(\frac{p'^2}{2k}-\mu\right)z'''} \times$$

$$\int_0^\infty rdrJ_m(pr)\ J_m(p'r)\,\rho(r,z') \quad . \tag{12}$$

For a Gaussian electron beam profile given by

$$\rho(r) = \frac{1}{2\pi\sigma^2}e^{-\frac{r^2}{2\sigma^2}} \ , \tag{13}$$

the transfer map in the spectral domain can be reduced to

$$\widetilde{K}_m(p,p',z,0) = -\frac{1}{2\pi}e^{-\frac{ip^2}{2k}z}\ \frac{\partial}{\partial\mu}\left[\int_0^z dz'\int_0^{z'} dz''\, e^{-i\left(\frac{p^2}{2k}-\mu\right)z'-i\left(\frac{p'^2}{2k}-\mu\right)z''}\right] \times$$

$$e^{-\frac{\sigma^2}{2}(p^2+p'^2)}\ I_m(\sigma^2\,pp') \ , \tag{14}$$

where I_m is the modified Bessel function of order m. Finally the spatial transfer map is related to the spectral transfer map by

$$K_m(r,r',z,0) = \int_0^\infty pdp\int_0^\infty p'dp'\,J_m(pr)\,J_m(p'r')\,\widetilde{K}_m(p,p',z,0) \ . \tag{15}$$

For numerical calculation, an appropriate boundary of the p-integration needs to be determined from the desired accuracy of the calculation [8].

It turns out that the transverse dependent part of the FEL map is a function of two parameters only, the resonance parameter ν, and an electron beam Fresnel number $F = 4\pi\sigma^2 / \lambda L$, as defined by Moore [9]. Once a map is generated, the FEL gain can still be varied through g_0.

For resonator calculation, the propagation from aperture 1 to aperture 2 in Fig.(1), which was the free-space Fresnel-Kirchhoff map in HOLD, has now the additional FEL map discussed in the above. The dominant mode is obtained by iterating the round-trip map obtained by combining the FEL map and the appropriate free-space maps. The advantage of this modular approach is that, given the electron beam and undulator parameters represented by ν and F, the FEL map can be generated once and for all, and stored for the subsequent calculations with various resonator configurations. Thus, the computing time can be greatly reduced. The resonator configuration is entirely general, including unstable resonators. Another approach based on the empty cavity mode expansion is reported in this conference to study the mode mixing effect duo to FEL gain in a hole-coupling resonator [10]. In this method, new map needs to be generated when the mirror curvature or the cavity length is changed. In addition, the unstable resonators can not be treated.

We have calculated the profile of the dominant mode and its gain for two-mirror resonators without holes for different values of the electron beam Fresnel number. At large Fresnel number, the fundamental mode has the highest gain, while a higher order mode becomes dominant at small Fresnel number. The results were compared with those of Moore [9], who obtained the profile of the maximum-gain mode, and found to agree well for large electron beam Fresnel number. The agreement is only qualitative for small Fresnel numbers, since Moore's maximum-gain mode in this regime requires a non-spherical mirror shape if it were considered as a resonator mode.

The transfer map approach developed here allows us to compute the gain as a function of the resonance parameter. Figure (4) shows the results for both amplifier and oscillator cases. For the amplifier case, the gain is obtained by passing the fundamental mode of an empty cavity without holes once through the gain medium. For the oscillator case, the gain is calculated for a new cavity mode obtained by iterating the round-trip transfer map starting from the same empty cavity mode. The sharp turning point on the oscillator gain curve is caused by a mode switching from the fundamental to next higher order empty cavity mode; As the electron beam becomes absorbing energy, the higher order mode which has smaller loss to the beam becomes dominant. Note here that the gain peaks near ν=4 rather than the well-known value from 1-D theory (ν=2.6). To stay close to the maximum gain,we will choose ν=4 for subsequent calculations.

Although the small signal condition is necessary for the analytical treatment of the FEL interaction, the techniques developed here are shown in the next section to be also applicable to the strong signal regime as long as the gain is low. The low gain assumption, on the other hand, is generally valid for an oscillator FEL which is meant to be operated at saturation. The high gain effects, such as optical guiding, are not important since they may occur only during a short turn-on period at small signal. A resonator optimized for the performance at saturation may not extract the highest gain at small signal. But this should not be a problem when there is enough gain for the laser to reach saturation.

4. Resonator Performance In the Presence of FEL Gain

The most striking influence of the FEL on the resonator mode appears to be the fact that the gain, even if small, can be very effective in suppressing the higher order modes among the azimuthally symmetric modes (m=0), when the electron beam Fresnel number is not too small. This is because the overlap with the electron beam is optimum for the fundamental mode. Figure (5.a), (5.b) and (5.c) show the intracavity mode profiles for a single pass gain of 0%, 2% and 55%, respectively. The resonator configuration is such that the dominant symmetric mode for 0% gain has a large mode number n=4. However, for a gain as small as 2%, the fundamental mode becomes dominant. Comparing Fig.(5.b) and Fig.(5.c), we find also that the mode profile changes little when the gain is varied from 2 to 55%. The hole coupling performance is therefore insensitive to the gain, except the desirable effect of suppressing the higher order symmetric modes. However it is preferable not to operate a laser only marginally staying away from the degeneracy. For example, when starting from a noisy profile in the Fox-Li calculation the iteration times it takes for the profile to converge to the fundamental mode is very large in the case of 2% gain as compared to the case of 55% gain. In this case, the difference in net gain between the fundamental and higher order mode becomes smaller as the FEL gain is reduced. It should be noted that the degeneracy is defined as two or more modes having the same net gain when a gain medium is introduced into an empty cavity.

As the electron beam Fresnel number becomes smaller, the higher order symmetric modes could become dominant. Operation with a higher order symmetric mode could provide a satisfactory hole coupling performance, since the mode has a narrow central peak and thus a good hole coupling efficiency. However, it will be usually necessary to suppress the higher order mode since the dominant resonator mode should not be allowed to switch from one mode to another while the FEL wavelength is being scanned. This can be accomplished by introducing the intracavity apertures.

It is expected that the asymmetric modes $m \neq 0$ will not be perturbed significantly due to FEL because their intensity vanish on axis at the electron beam location. The study with FEL map confirms this. Therefore the asymmetric modes should be studied and controlled, especially at a large hole size. The situation is similar to the empty cavity case. The solution is also similar; The asymmetric higher order modes are suppressed by means of adjustable intracavity aperture.

In calculating the performance of an FEL oscillator, the electron beam size is determined by its emittance and the natural focussing of the undulator, assuming a round beam matched to the helical undulator. The undulator parameter K is determined for each wavelength by the FEL resonance condition. These parameters then determine the value of the gain parameter g_0 given by Eq.(6). As the intensity increases in the oscillator, the gain decreases from pass to pass. The saturated value of the gain G_S at steady state is given by

$$(1 - \alpha_T)(1 + G_S) = 1. \tag{16}$$

The mode profile and the resonator performance at saturation may therefore be obtained by computing the dominant mode for a sequence of decreasing values of g_0 until the above equation is satisfied. The results was compared with those obtained by the oscillator version [11] of the three-dimensional FEL simulation code TDA [12]. The agreement is excellent when the saturated gain is

resonators with holes on axis", these proceedings.

[11] S. Krishnagopal, M. Xie, K.-J. Kim and A. Sessler, "Three-Dimensional Simulation of a Hole-Coupled FEL Oscillator", these proceedings.

[12] T.M. Tran and J. Wurtele, Comp. Phys. Comm. 54 (1989) 263.

Table 1. Norminal Parameters Used in the Calculations

Cavity Length [m]	8.2
Mirror Radius of Curvature [m]	4.3
Radius of the Right Mirror [mm]	15
Radius of the Left Mirror [mm]	6.7 - 15
Hole Radius [mm]	0.8
Radius of Apertures [mm]	8
Aperture Separation [m]	2
Undulator Length [m]	2
Undulator Period [cm]	5
Undulator Parameter (K)	0.637 - 1.35
Beam Energy [MeV]	55.3
Beam size (σ) [mm]	0.4 - 0.6
Normalized rms beam emittance [mm-mrad]	20

Figure Captions

Figure 1. Cross-sectional view of the cylindrical resonator consisting of two mirrors and two intracavity apertures. A circular hole is placed at the center of the right mirror. An adjustable aperture is placed in front of the left mirror for mode control. The dashed lines indicate the boundary of an undulator bore simulated by two fixed apertures. An electron beam traverses the FEL interaction region from aperture 1 to aperture 2.

Figure 2. Hole coupling performance at different wavelengths. The radius of the left mirror is increased linearly from 6.7 mm to 10 mm as the wavelength is varied from 3 to 6 μm.

Figure 3. Same as Fig.2 except the radius of the left mirror is fixed at 8.35 mm for all the wavelengths.

Figure 4. The gain curves for the amplifier and the oscillator cases at 3 μm wavelength. There are no holes on the cavity mirrors. The radius of the left mirror is 15 mm.

Figure 5. Intracavity intensity profiles of the dominant mode at 3 μm wavelength with a gain of (a) 0%, (b) 2%, and (c) 55%.

Figure 6. Hole coupling performance of the TEM_{00} mode with intracavity FEL gain, the left mirror radius is 7, 8.3, 9.4 and 10.3 mm at 3, 4, 5 and 6 μm wavelength, respectively.

Figure 7. The net gains of the TEM_{00} and TEM_{10} mode at small signal and saturation for the same resonators as Fig.(6).

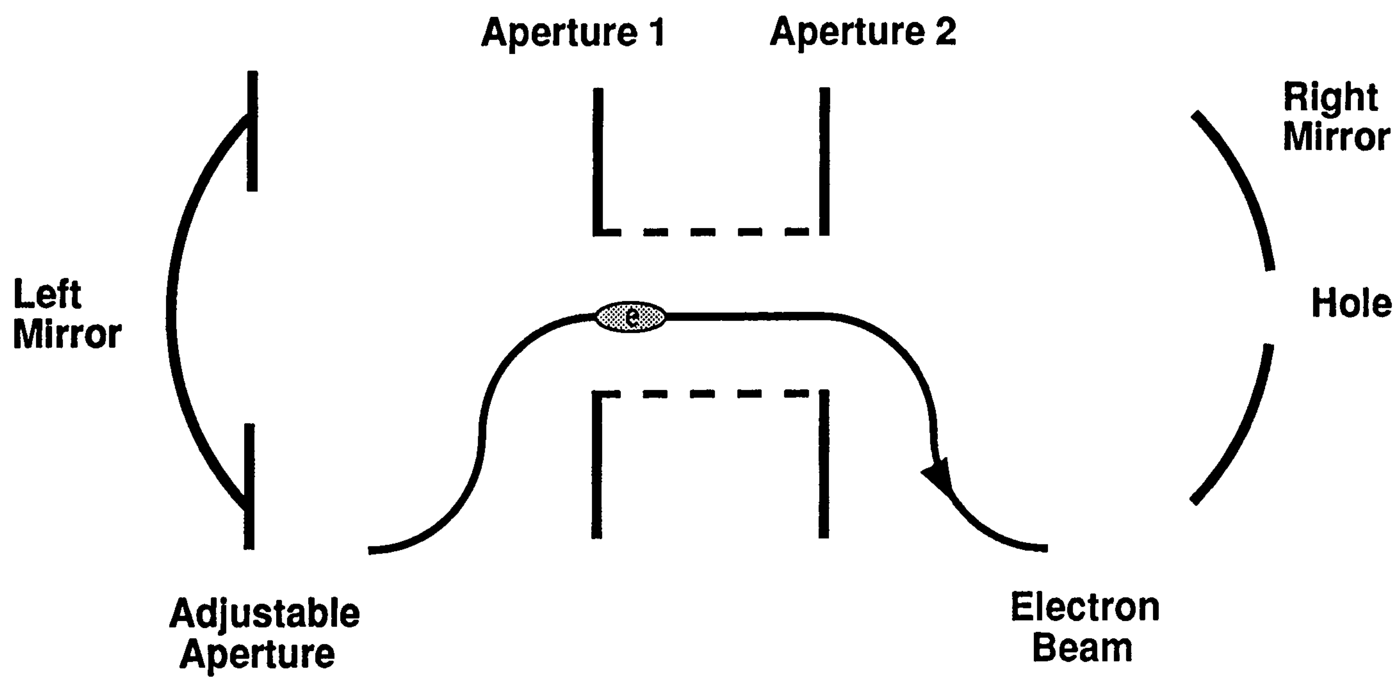

Aperture 1
Aperture 2
Right
Mirror
Left
Mirror
e
Hole
Adjustable
Aperture
Electron
Beam

Figure 1

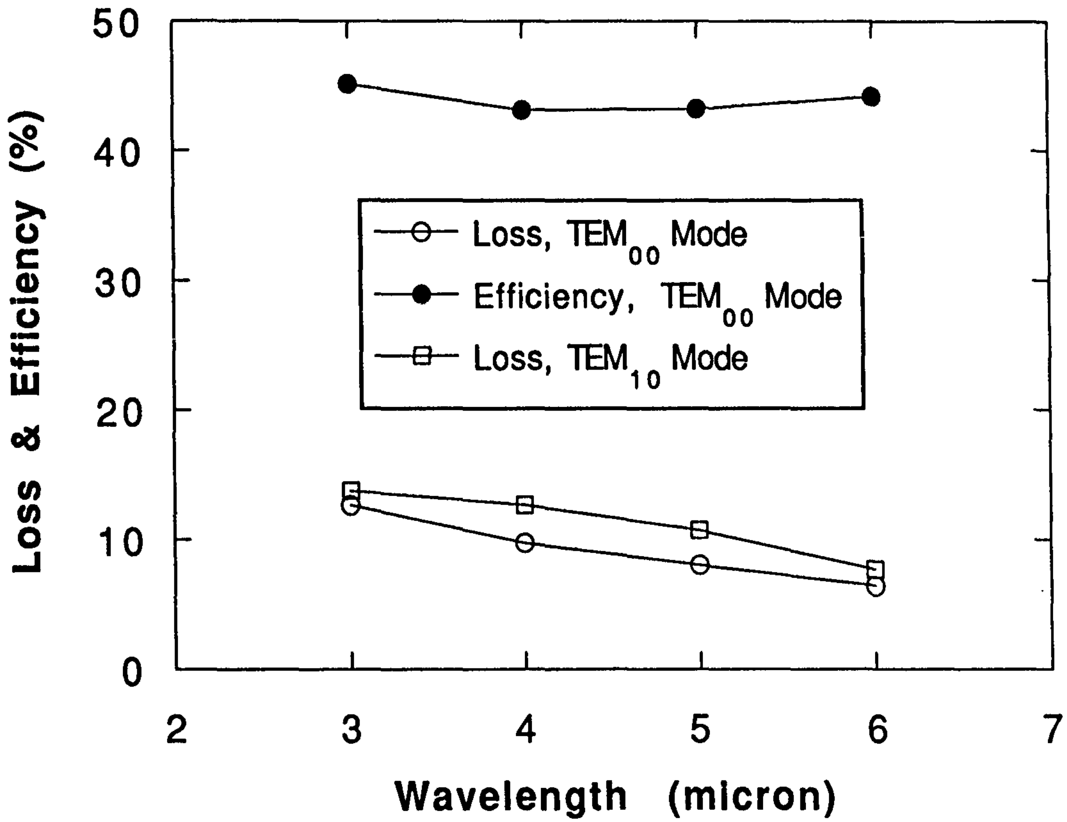

Loss & Efficiency (%)
50
40
30
20
10
0
Loss, TEM00 Mode
Efficiency, TEM00 Mode
Loss, TEM10 Mode
2
3
4
5
6
7
Wavelength (micron)

Figure 2

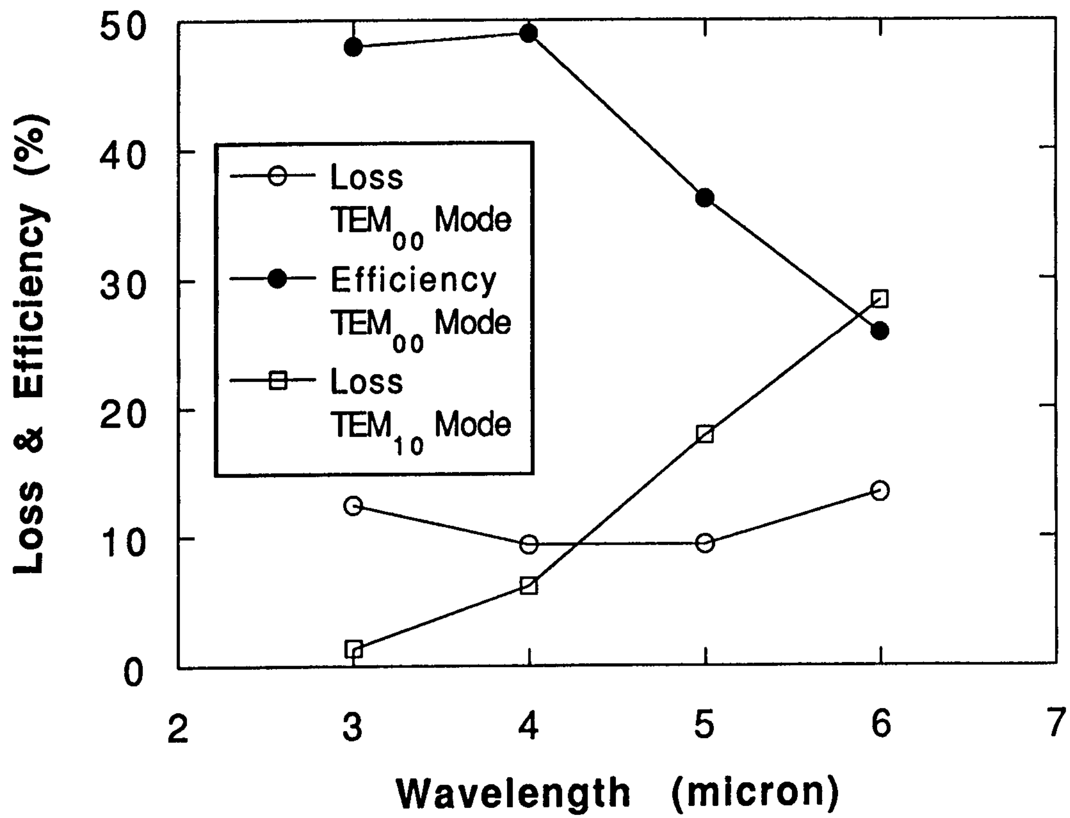

Loss & Efficiency (%)
Wavelength (micron)
0
10
20
30
40
50
2
3
4
5
6
7
Loss
TEM00 Mode
Efficiency
TEM00 Mode
Loss
TEM10 Mode

Figure 3

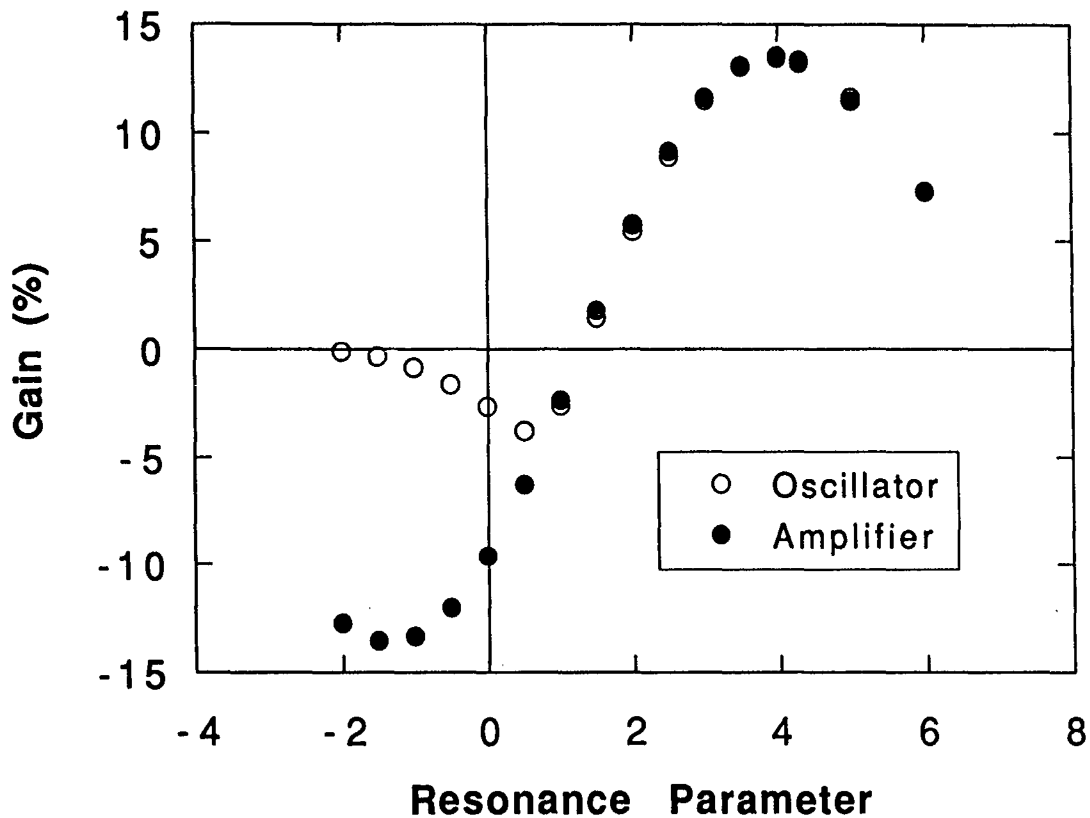
15
10
5
0
-5
-10
-15
Gain (%)
-4
-2
0
2
4
6
8
Resonance Parameter
Oscillator
Amplifier

Figure 4

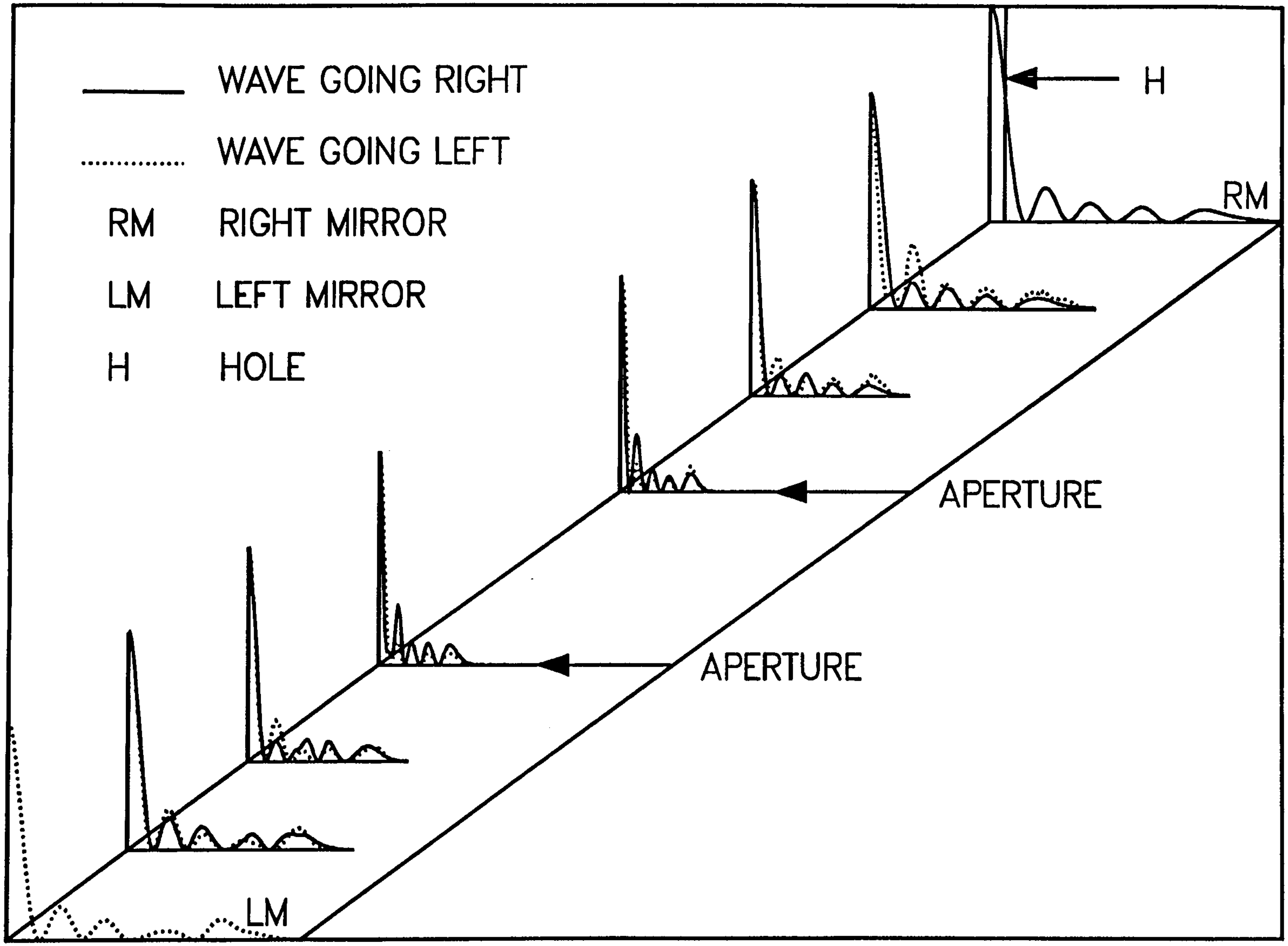
WAVE GOING RIGHT
WAVE GOING LEFT
RM RIGHT MIRROR
LM LEFT MIRROR
H HOLE
H
RM
APERTURE
APERTURE
LM

Figure 5.a

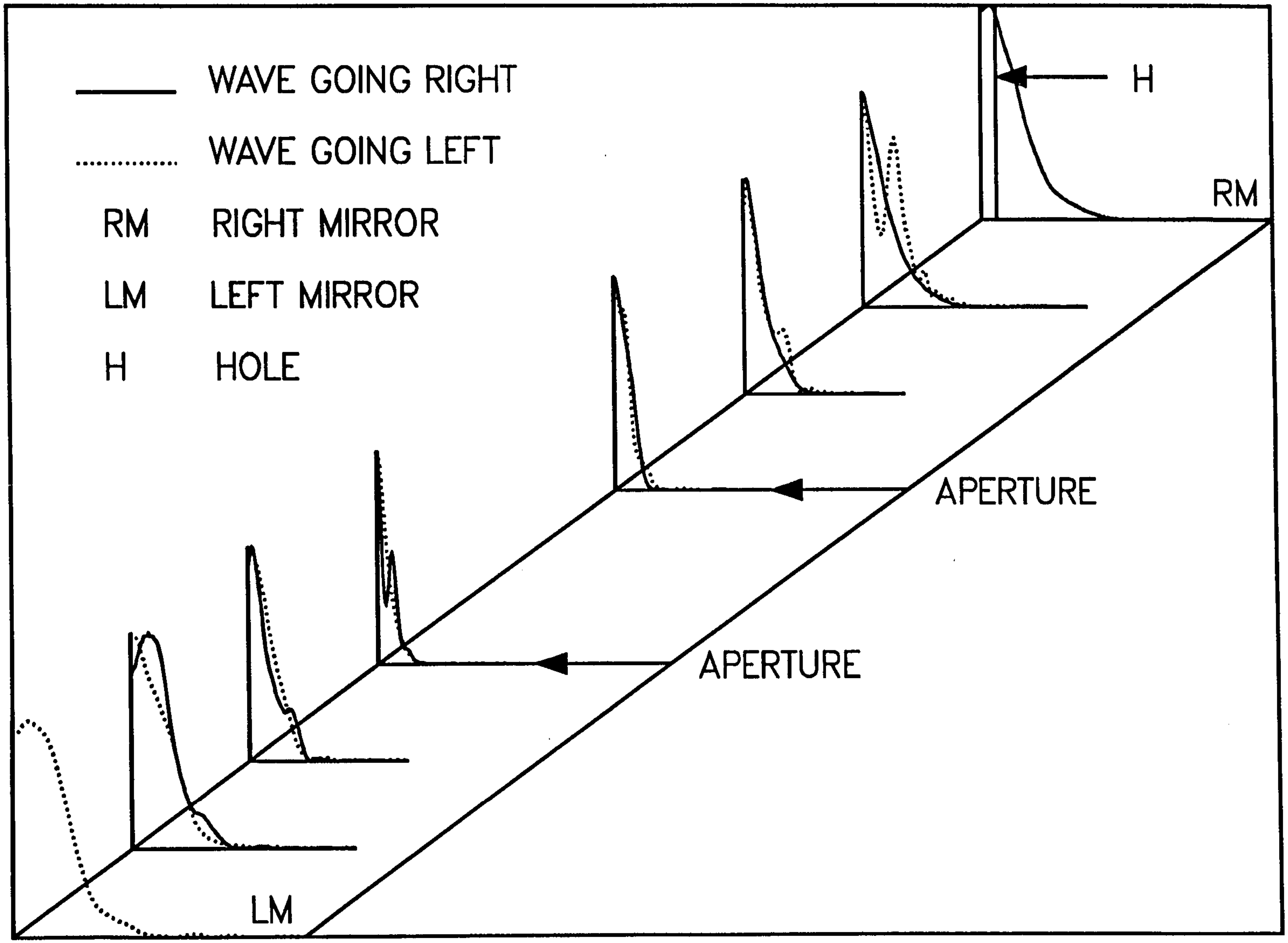
WAVE GOING RIGHT
WAVE GOING LEFT
RM
RIGHT MIRROR
LM
LEFT MIRROR
H
HOLE
H
RM
APERTURE
APERTURE
LM

Figure 5.b

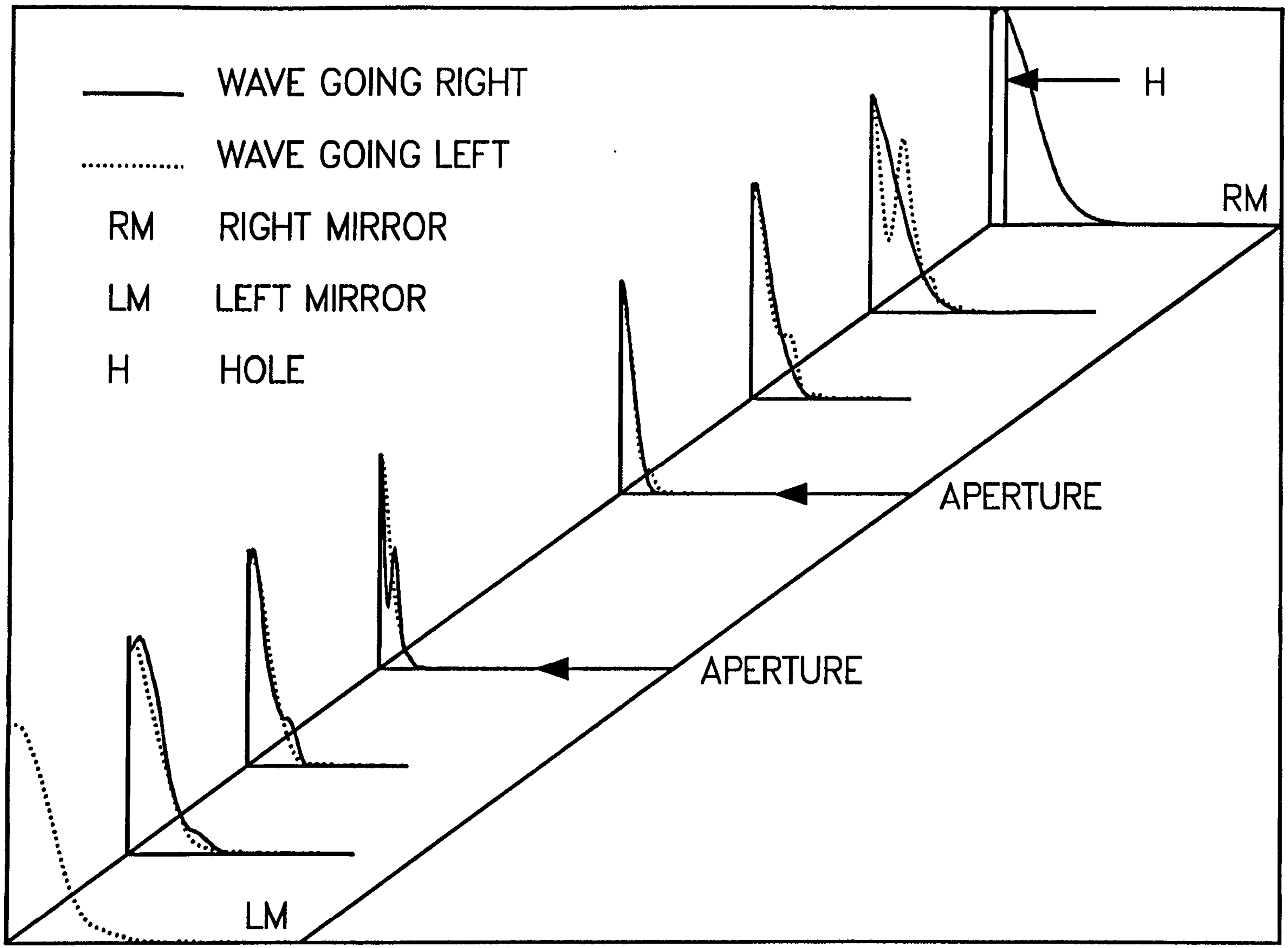
WAVE GOING RIGHT
WAVE GOING LEFT
RM RIGHT MIRROR
LM LEFT MIRROR
H HOLE
H
RM
APERTURE
APERTURE
LM

Figure 5.c

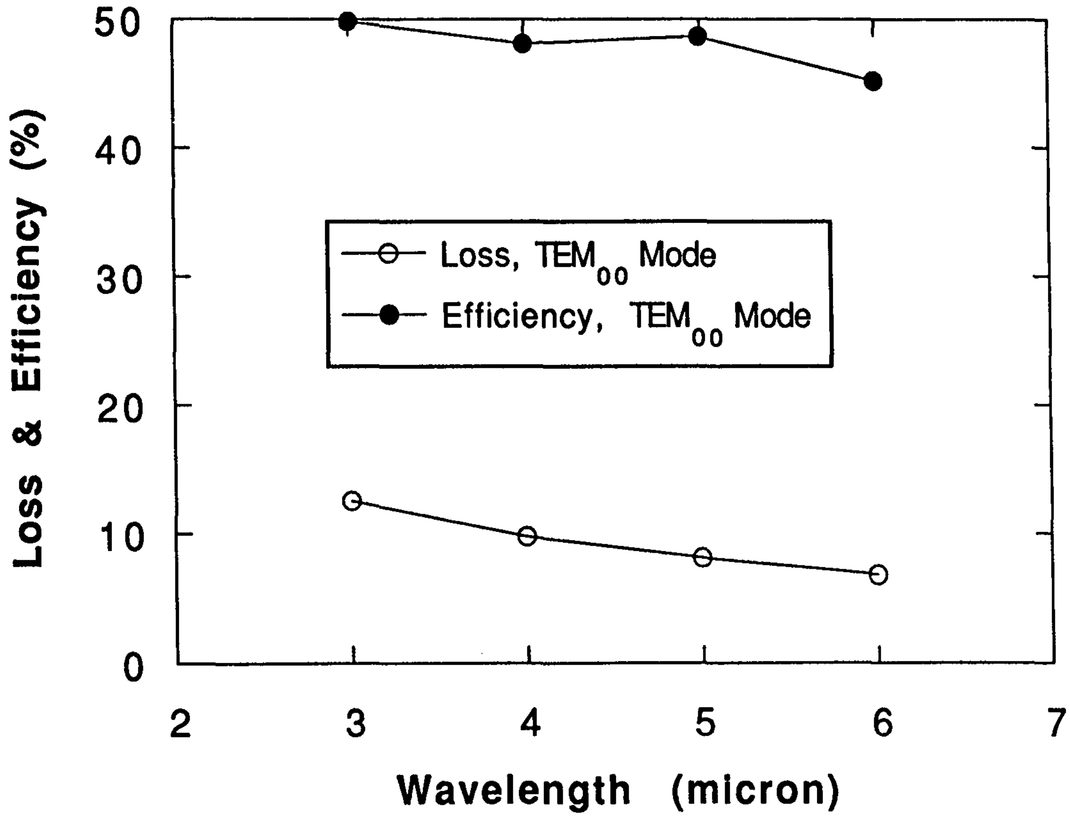

Loss & Efficiency (%)
0
10
20
30
40
50
2
3
4
5
6
7
Wavelength (micron)
Loss, TEM00 Mode
Efficiency, TEM00 Mode

Figure 6

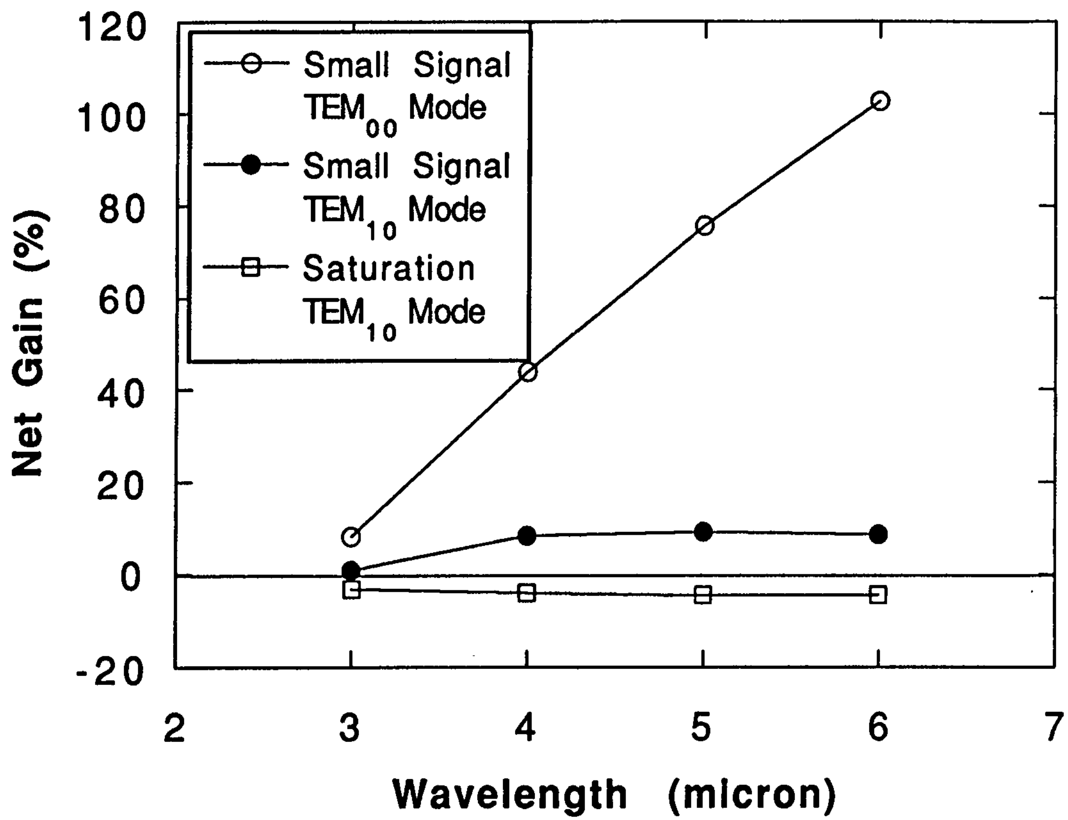

Small Signal TEM00 Mode
Small Signal TEM10 Mode
Saturation TEM10 Mode
120
100
80
60
40
20
0
-20
Net Gain (%)
2
3
4
5
6
7
Wavelength (micron)

Figure 7